JULY 12–16 2020 VIRTUAL JOINT AAPM | COMP MEETING
EASTERN TIME [GMT-4]

The Relationship Between Beam Width, Scan Length, and Dosimeter Dimension in CT Equilibrium Dose Measurements

V Weir[1], J Zhang[2]

1. Baylor University Medical Center, Plano, TX
2. University of Kentucky, Lexington, KY

INTRODUCTION

In conventional computed tomography (CT) scanning, doses can be measured at z = 0 in a CT phantom of "infinite" length, for a given scan length. At longer scan lengths, the dose measured by the detector reaches an asymptote measurement called $D_{eq,}$ and returns the same measurement value at scan lengths *L* greater than a quantity called the equilibrium scan length L_{eq}. In wide beam or cone-beam CT, when a detector is placed in a CT phantom of infinite length, the central ray dose $f(0)_a$, measured at the peak (z=0) of the dose profile function for some beam width, *a(nT)*, increases with the beam width until reaching an asymptote [1]. The approach to equilibrium of these doses under increasing beam widths, *a,* or scan lengths, *L*, in an infinite phantom can be described by a mathematical growth model. An infinite phantom is long enough to allow the dose profile to converge to zero at the ends of the phantom. Minimally, if the dose measured by a detector placed at z = 0 is to be called the equilibrium dose, D_{eq}, we need to know the equilibrium scan length L_{eq}.

Although there is currently extensive discussion on how to obtain D_{eq} for dose measurements [4], it is not clear how to obtain L_{eq} for dose measurements at any given beam width. This is to say it is not clear what the minimum phantom length should be so as to allow the dose profile to converge at a given beam width. A simple approach for accurately determining L_{eq} is to model the effect, on measured dose, of minimum ion chamber detector lengths, *d*, at different beam widths in order to determine a relationship which can then be used to derive L_{eq}. In previous studies where L_{eq} was obtained, the scan length was used as a variable in the approach-to-equilibrium function [1], or a 900-mm-long phantom was scanned at different beam widths [5], and L_{eq} was read off a graph of the dose profile function. L_{eq} has also been obtained using Monte Carlo simulations where different scan lengths were considered [6-8].

The aforementioned studies did not report the effects of the measuring detector length or the relationship between the beam width and the detector length on the approach-to-equilibrium function.

AIM

AAPM TG#111 proposed the equilibrium dose to address the concern of wide beam CT dose measurement. The just-published TG#200 detailed the implementation of this approach. This study is to elucidate, theoretically and experimentally, the relationship between x-ray beam width, scan length, and dosimeter dimension for accurate equilibrium dose measurement.

METHOD

The equilibrium dose was modeled as an approach-to-equilibrium function which is typically presented as growth functions. Accordingly, two ordinary differential equations (ODEs) were derived to simulate two scenarios: varying x-ray beam width with a fixed active dosimeter size and a fixed beam width with varying dosimeter size (integration length). Both cases were validated in a 256-slice CT scanner with a 60-cm body phantom. The beam widths were set at 5, 40, 80, 120, 140, and 160 mm (Figure 1) , respectively, and the integrating detectors were set as 10, 20, 30, 40, 50, 60, 100mm (Figure 2) for each beam width.

Eight sleeves were constructed and placed in different arrangements (Figure 3) to create dosimeter sizes of 10, 20, 30, 40, 50, 60 mm, and 100mm (no sleeve) on a 100mm pencil chamber. The ratio of the beam width to the dosimeter size was used to predict the minimum beam width, while the minimum dosimeter length was the one that integrated 98% of exposure.

METHOD

We construct an initial value problem (IVP) with beam width *a* (in this case z) as variable as below, where d/α is a parameter called length constant and H is the dose (mGy) measured at the peak (central ray dose)

$$\frac{d}{\alpha}y' + y - H = 0 \quad z \in [5,40,80,120,140,160]$$

With the initial condition $y(0) = H_{min}$, a general solution is

$$y(z) = k_1 e^{-\frac{\alpha z}{d}} + H$$

This results in the solution we call the model for figure 1

$$y(z) = H\left(1 - e^{-\frac{\alpha z}{d}}\right) + H_{min}e^{-\frac{\alpha z}{d}}$$

We construct a second initial value problem (IVP) with sleeve gap d as the variable as below, where a/α is a parameter called length constant and H is the dose (mGy) measured at sleeve gap

$$\frac{a}{\alpha}y' + y - H = 0 \; d \in \{10, 20, 30, 40, 50, 60, 100\}$$

With the initial condition $y(0) = H_{min}$, a general solution is

$$y(d) = k_1 e^{-\frac{\alpha d}{a}} + H$$

This results in the solution we call the model for figure 2

$$y(d) = H\left(1 - e^{-\frac{\alpha d}{a}}\right) + H_{min}e^{-\frac{\alpha d}{a}}$$

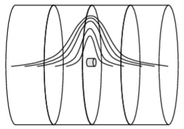

Figure 1. *Point detector and different beam widths. Point detector is represented by a sleeve gap on the pencil chamber. Each point detector was placed at center and periphery, and peak dose at the center of a beam width measured. This was done for each beam width from 5mm – 160mm then the width of the sleeve gap changed, and the process repeated for 10mm to 100mm sleeve gaps.*

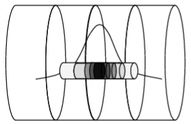

Figure 2. *Integrating detector and same beam width. Integrating detector is represented by widening the sleeve gap on the pencil chamber from the narrowest to the widest sleeve gap (10mm …100mm) while integrating a given beam . Different beam widths were integrated in this way until all beam widths were measured.*

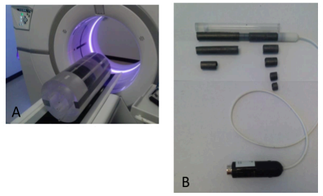

Figure 3. *(A) 60-cm-long body phantom and (B) Pencil chamber with various lead sleeves used for creating the sleeve gaps.*

RESULTS

The model is translated into familiar notation by replacing the variable *y(z)* by the central ray dose, $f(0)_a$, measured at the peaks of the dose profile, and replacing *H* by the f_{eq}. For figure 1 we have

$$f(0)_a = f_{eq}\left(1 - e^{-\frac{\alpha a}{d}}\right) + H_{min}e^{-\frac{\alpha a}{d}}$$

While for figure 2 we have

$$y(d) = H\left(1 - e^{-\frac{\alpha d}{a}}\right) + H_{min}e^{-\frac{\alpha d}{a}}$$

Tables 1 & 2 show the results tabulated for data related to figures 4 & 5. Table 3 shows the results of linear regression analysis showing a good correlation between the measurement and the proposed equation (R^2 is from 0.96 to 0.99) at all beam widths except the smallest beam width of 5 mm. The modeling results also show that the minimum dosimeter length *d* for integrating 98% of the signal for a given beam width *a* is $d = 5.01a$ (for 160mm beam width in table 2). Further analysis shows that the minimum beam width *a*, at which a dosimeter of length *d* is used as a point dosimeter, is $a = 4.99d$ (for 100 mm sleeve gap in table1).

Another important result is that the Farmer chamber data fits into the data for lead sleeves, Figure 6, suggesting that there is the possibility to use lead sleeves around a pencil chamber to measure point doses when the appropriate sleeve gap is used.

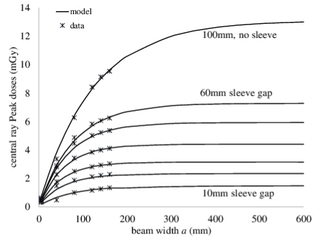

Figure 4*. doses measured at the peak (peak doses) vs. beam width for a 256-slice GE Revolution CT scanner. The peak dose at each beam width is collected at different sleeve gaps of 10, 20, 30, 40, 50, 60, and 100 mm (pencil chamber with no plastic cover).*

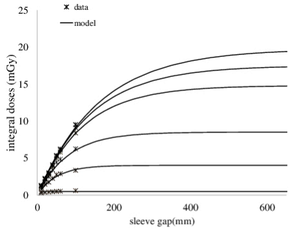

Figure 5*. Integral dose vs. sleeve gap d(mm) for a 256-slice GE Revolution scanner. The dose at each sleeve gap is collected at different beam widths of 5, 40, 80, 120, 140, and 160 mm. The highest dose occurs at the beam width of 160 mm, and the lowest occurs at 5 mm.*

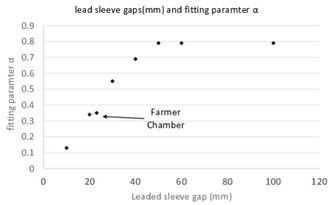

Figure 6*. Fitting parameters and various sleeve gaps showing the relationship up to 100mm sleeve gaps. Data showing the location of a Farmer chamber relative to sleeve gap data is also represented.*

Table 1*. Fitting parameters are shown at different sleeve gaps (surrogate detector dimension). The beam width a at which an integrating detector of dimension equal to the sleeve gap will behave as a point detector is also shown.*

Sleeve gap d (mm)	A	Dose (5mm beam width /d) from fits to fig.4	Beam Width (a) (mm)*
10	0.13	1.046	a=30.36d
20	0.34	1.1303	a=11.61d
30	0.55	1.0627	a=7.18d
40	0.69	1.0627	a=5.72d
50	0.79	1.0725	a=4.99d
60	0.79	1.0627	a=4.99d
100	0.79	1.0361	a=4.99d

RESULTS

Table 2*. For each beam width selected in the first column, the fitting parameter α is shown in the second column. The fourth column shows a formula for length of sleeved chamber needed to collect 98% of the signal. This is for data collected in a 60 cm long body phantom at both central and peripheral positions using the technique factors stated earlier.*

Beam width a(mm)	α	Dose (10mm sleeve gap/a) from fits to fig.5	Relation between d and a(mm)	Minimum detector length d (mm)	Minimum phantom length a_{eq} (mm)*	Equilibrium scanning length L_{eq} (mm)**
5	0.89	1	d=4.4a	21.9	21.9	21.9
40	0.79	1.2184	d=5.2a	208.0	208.0	208.0
80	0.79	1.1038	d=5.08a	406.4	406.4	406.4
120	0.79	1.068	d=5.04a	604.8	604.8	604.8
140	0.79	1.0581	d=5.02a	702.8	702.8	702.8
160	0.79	1.0506	d=5.01a	801.6	801.6	801.6

Table 3*. Evaluation of the model by linear regression. Experimental Exposure at different sleeve gaps for a fixed beam width*

Collimation	Linear regression	R^2	RMSE
5	y=0.1764x+44.448	0.5625	0.067825
40	y=1.0249x	0.9606	0.19666
80	y=0.993x	0.9848	0.227744
120	y=1.0069x	0.9949	0.176914
140	y=1.0217x	0.9935	0.215706
160	y=1.0148x	0.9947	0.202454

CONCLUSIONS

An initial value problem based on an ODE yields a solution that provides a better understanding of the relationship between beam width, scan length and dosimeter size for wide beam CT equilibrium dose measurements. The model reveals that for peak-dose measurements the beam width *a* should be at least five times longer than the detector length *d*. For integral dose measurements the detector length *d* and therefore, the minimum phantom length $a_{eq,}$ should be at least five times longer than the beam width *a*.

REFERENCES

1. Dixon, R.L. and J.M. Boone, *Cone beam CT dosimetry: A unified and self-consistent approach including all scan modalities—With or without phantom motion.* Medical Physics, 2010. 37(6): p. 2703-2718.
2. AAPM, *Comprehensive Methodology for the evaluation of Radiation Dose in X-Ray Computed Tomography, : February 2010.* , in *The Future of CT Dosimetry*2010, AAPM TG 111.
3. Weir, V.J., *A model of CT dose profiles in Banach space; with applications to CT dosimetry.* Physics in Medicine and Biology, 2016. 61(13): p. 5020.
4. Gomà, C., et al., *Radiation dose assessment in a 320-detector-row CT scanner used in cardiac imaging.* Medical Physics, 2011. 38(3): p. 1473-1480.
5. Mori, S., et al., *Enlarged longitudinal dose profiles in cone-beam CT and the need for modified dosimetry.* Medical Physics, 2005. 32(4): p. 1061-1069.
6. Li, X., D. Zhang, and B. Liu, *Monte Carlo assessment of CT dose equilibration in PMMA and water cylinders with diameters from 6 to 55 cm.* Medical Physics, 2013. 40(3): p. 031903.
7. Zhou, H. and J.M. Boone, *Monte Carlo evaluation of CTDI∞ in infinitely long cylinders of water, polyethylene and PMMA with diameters from 10 mm to 500 mm.* Medical Physics, 2008. 35(6): p. 2424.
8. Boone, J.M., *Dose spread functions in computed tomography: a Monte Carlo study.* Medical Physics, 2009. 36(10): p. 4547-4554.

CONTACT INFORMATION

Victor Weir, vjweir@gmail.com.